Ulusal ROMATOLOJİ Dergisi
Journal of Turkish Society for Rheumatology www.romatolojidergisi.org

Original Article / Orijinal Araştırma

DOI: 10.4274/raed.galenos.2026.92905
J Turk Soc Rheumatol

Cardiac MRI patterns in cardiac amyloidosis vs. non-amyloid inflammatory and fibrotic cardiac involvement: A single-center pilot study

Kardiyak amiloidoz ile non-amiloid enflamatuvar ve fibrotik kardiyak tutulumda kardiyak MRG paternleri: Tek merkezli pilot çalışma

Göksel Tuzcu, Ali Alkaşi

Aydın Adnan Menderes University Faculty of Medicine, Department of Radiology, Aydın, Türkiye

Abstract

Objective: Cardiac amyloidosis (CA) is an infiltrative cardiomyopathy that various non-amyloid inflammatory and fibrotic cardiac diseases with overlapping clinical features can mimic. This study aims to compare cardiac magnetic resonance imaging (CMR) patterns between these conditions to identify imaging features that facilitate accurate differential diagnosis.

Methods: This single-center, retrospective, pilot comparative study included 27 patients who underwent CMR between December 2021 and November 2025. Fourteen patients had confirmed CA and 13 patients had non-amyloid inflammatory or fibrotic cardiac involvement, including cardiac sarcoidosis, connective tissue disease-related cardiac involvement, inflammatory myocarditis, systemic sclerosis, and endocardial fibroelastosis. All CMR examinations were performed on a 1.5-T magnetic resonance imaging system using a standardized protocol. Imaging parameters included left ventricular wall thickness, atrial size, presence of pericardial or pleural effusion, late gadolinium enhancement (LGE) patterns, and myocardial edema on T2-weighted imaging. Groups were compared using appropriate parametric or non-parametric statistical tests, as applicable.

Results: Patients with CA were older than the non-amyloid group (51.7±13.8 vs. 36.6±13.4 years, p=0.008). Biatrial dilatation was more frequent in CA (71.4% vs. 15.4%, p=0.006), whereas pericardial and pleural effusions were more common in the non-amyloid group (61.5% vs. 14.3%, p=0.018; and 53.8% vs. 14.3%, p=0.046, respectively). Diffuse subendocardial LGE was strongly associated with CA (64.3% vs. 0%, p<0.001). In contrast, the non-amyloid group more frequently demonstrated transmural (84.6% vs. 21.4%, p=0.002), patchy (61.5% vs. 7.1%, p=0.004), mid-myocardial (76.9% vs. 14.3%, p=0.002), and subepicardial LGE patterns (84.6% vs. 0%, p<0.001). Myocardial edema on T2 mapping was observed only in the non-amyloid group (30.8% vs. 0%, p=0.041).

Conclusion: CMR reveals distinct and reproducible imaging patterns that enable differentiation of CA from non-amyloid inflammatory and fibrotic cardiac diseases. A pattern-based CMR approach may improve diagnostic confidence and support disease-specific clinical management, even in small, real-world cohorts.

Keywords: Cardiac amyloidosis, cardiac magnetic resonance, differential diagnosis, inflammatory cardiomyopathy, late gadolinium enhancement

Özet

Amaç: Kardiyak amiloidoz (KA), çeşitli non-amiloid enflamatuvar ve fibrotik kardiyak hastalıkların benzer klinik özelliklerle taklit edebildiği infiltratif bir kardiyomiyopatidir. Bu çalışmada, bu durumlar arasında ayırıcı tanıyı kolaylaştırabilecek görüntüleme bulgularını belirlemek amacıyla kardiyak manyetik rezonans görüntüleme (KMR) paternlerinin karşılaştırılması amaçlandı.

Yöntem: Bu tek merkezli, retrospektif, pilot karşılaştırmalı çalışmaya Aralık 2021-Kasım 2025 tarihleri arasında KMR yapılan 27 hasta dahil edildi. On dört hastada KA tanısı doğrulanmıştı; 13 hastada ise kardiyak sarkoidoz, bağ dokusu hastalığı ilişkili kardiyak tutulum, enflamatuvar miyokardit, sistemik skleroz ve endokardiyal fibroelastozisi içeren non-amiloid enflamatuvar/fibrotik kardiyak tutulum mevcuttu. Tüm KMR incelemeleri 1,5-T cihazda standart protokol ile gerçekleştirildi. Sol ventrikül duvar kalınlığı, atriyal boyutlar, perikardiyal/plevral efüzyon varlığı, geç gadolinyum tutulumu (LGE) paternleri ve T2 ağırlıklı görüntülerde miyokardiyal ödem değerlendirildi. Gruplar uygun parametrik veya non-parametrik testlerle karşılaştırıldı.

Bulgular: KA grubundaki hastalar non-amiloid gruba göre daha yaşlıydı (51,7±13,8 vs. 36,6±13,4 yıl; p=0,008). Biatriyal dilatasyon KA grubunda daha sıktı (%71,4 vs. %15,4; p=0,006). Buna karşılık perikardiyal ve plevral efüzyon non-amiloid grupta daha sık izlendi (%61,5 vs. %14,3; p=0,018 ve %53,8 vs. %14,3; p=0,046). Diffüz subendokardiyal LGE, KA ile güçlü ilişki gösterdi (%64,3 vs. %0; p<0,001). Non-amiloid grupta ise transmural (%84,6 vs. %21,4; p=0,002), yamalı/patchy (%61,5 vs. %7,1; p=0,004), mid-miyokardiyal (%76,9 vs. %14,3; p=0,002) ve subepikardiyal LGE paternleri (%84,6 vs. %0; p<0,001) daha sık görüldü. T2 mapping ile miyokardiyal ödem yalnızca non-amiloid grupta saptandı (%30,8 vs. %0; p=0,041).

Sonuç: KMR, KA'yı non-amiloid enflamatuvar ve fibrotik kardiyak hastalıklardan ayırt etmeye yardımcı olan belirgin ve tekrarlanabilir görüntüleme paternleri ortaya koymaktadır. Patern temelli KMR değerlendirmesi, küçük ve gerçek yaşam kohortlarında dahi tanısal güveni artırabilir ve hastalığa özgü klinik yönetimi destekleyebilir.

Anahtar Kelimeler: Kardiyak amiloidoz, kardiyak manyetik rezonans, ayırıcı tanı, enflamatuvar kardiyomiyopati, geç gadolinyum tutulumu

Correspondence / İletişim: Asst. Prof. Dr. Göksel Tuzcu;
Aydın Adnan Menderes University Faculty of Medicine, Department of Radiology, Aydın, Türkiye
E-mail: gokseltuzcu@gmail.com ORCID ID: orcid.org/0000-0002-3957-1770
Received / Geliş Tarihi: 14.01.2026 Accepted / Kabul Tarihi: 12.03.2026 Epub: 16.03.2026

Cite this article as / Atıf: Tuzcu G, Alkaşi A. Cardiac MRI patterns in cardiac amyloidosis vs. non-amyloid inflammatory and fibrotic cardiac involvement: a single-center pilot study. J Turk Soc Rheumatol. [Epub Ahead of Print]

Introduction

Cardiac amyloidosis (CA) is an infiltrative cardiomyopathy characterized by extracellular deposition of misfolded amyloid fibrils within the myocardial interstitium, leading to progressive myocardial stiffening, restrictive physiology, heart failure, and a poor prognosis.[1-3] Because clinical presentation is often nonspecific and overlaps with other causes of myocardial thickening, CA may remain underrecognized, particularly in early disease. Timely identification has become increasingly important with the availability of disease-modifying therapies, especially for transthyretin-related amyloid cardiomyopathy.[4,5]

In rheumatology practice, systemic inflammatory diseases may involve the myocardium through inflammation and/or fibrosis and can mimic infiltrative phenotypes on imaging. CA, inflammatory myocarditis in systemic lupus erythematosus (SLE), rheumatoid arthritis-related myocardial involvement, systemic sclerosis, and rare fibrotic entities may present with heart failure symptoms and arrhythmias and may show myocardial enhancement on cardiac magnetic resonance (CMR).[6-9] Although these conditions can share overlapping clinical and imaging findings, their pathophysiology differs fundamentally from amyloid deposition, and this difference is expected to translate into distinct tissue characterization profiles on CMR.

CMR enables comprehensive non-invasive evaluation of myocardial morphology and tissue characterization. In particular, the distribution of late gadolinium enhancement (LGE), assessment of myocardial edema (including T2 mapping), and associated morphological features may provide practical clues for differential diagnosis in real-world clinical settings.[8,10-12] However, direct comparative data contrasting CA with a spectrum of non-amyloid inflammatory and fibrotic myocardial involvement remain limited.

The objective of this single-center pilot study was to compare CMR patterns in patients with CA and those with non-amyloid inflammatory or fibrotic cardiac involvement, and to identify imaging features, particularly LGE distribution, myocardial edema on T2 mapping, and relevant morphological findings, that facilitate accurate differential diagnosis.

Materials and Methods

Study Design and Setting

This was a single-center, retrospective, pilot comparative study conducted in accordance with the Declaration of Helsinki. Ethical approval was obtained from the Non-Interventional Clinical Research Ethics Committee of Aydın Adnan Menderes University Faculty of Medicine (approved number: 07-2025/377, date: 18.12.2025). Informed consent was waived due to the retrospective design and use of anonymized data.

Study Population and Group Definitions

Consecutive patients who underwent CMR for suspected infiltrative or inflammatory cardiac disease between December 2021 and November 2025 were identified from the institutional imaging archive and electronic medical record system. Patients were included if they had diagnostic-quality CMR and a confirmed diagnosis of either CA or non-amyloid inflammatory/fibrotic cardiac involvement based on clinical evaluation and supporting diagnostic investigations.

Cardiac Amyloidosis Group

The CA group included patients with a confirmed diagnosis of CA (n=14) established by cardiology/hematology assessment using disease-specific criteria supported by clinical, laboratory, and imaging findings (and histopathology when available).

Non-Amyloid Inflammatory/Fibrotic Group

The comparison group included patients with inflammatory or fibrotic myocardial involvement unrelated to amyloid deposition (n=13), comprising cardiac sarcoidosis (n=5), rheumatoid arthritis–related cardiac involvement (n=3), SLE-associated myocarditis (n=3), systemic sclerosis (n=1), and endocardial fibroelastosis (n=1). Given the limited number of patients within each diagnosis, subgroup analyses were reported descriptively.

Exclusion Criteria

Patients were excluded if CMR image quality was non-diagnostic (e.g., severe motion artifacts), key clinical/imaging data were unavailable, or the examination was incomplete for tissue characterization.

CMR Acquisition

All CMR examinations were performed on a 1.5-T system (Achieva; Philips Healthcare, Best, the Netherlands) using a standardized institutional protocol. The protocol included:

(i) cine steady-state free precession (SSFP) sequences acquired in standard long-axis and contiguous short-axis planes for assessment of cardiac morphology and ventricular function;

(ii) T1-weighted imaging;

(iii) T2 mapping for evaluation of myocardial edema, when clinically indicated; and

(iv) LGE imaging.

A gadolinium-based contrast agent was administered intravenously at a dose of 0.1 mmol/kg. LGE images were acquired 10-15 minutes after contrast administration using phase-sensitive inversion recovery sequences.

Image Analysis

All CMR images were independently reviewed by two radiologists experienced in cardiac imaging, who were blinded to clinical diagnoses and laboratory data. Final interpretations were reached by consensus.

The following parameters were systematically assessed:

- Maximum left ventricular wall thickness,
- Left and right atrial size (presence of biatrial dilatation),
- Presence of pericardial and/or pleural effusion,
- Presence and distribution of LGE,
- Evidence of myocardial edema on T2-weighted imaging (present/absent).

LGE Pattern Classification

LGE distribution was classified by visual assessment according to the predominant location within the myocardial wall and the extent of involvement. Enhancement was categorized as subendocardial, mid-myocardial, subepicardial, or transmural when it predominantly involved the corresponding myocardial layer. A pattern was considered diffuse when enhancement involved multiple segments in a circumferential or widespread manner, whereas patchy enhancement referred to focal or multifocal non-contiguous areas of LGE. LGE patterns were not mutually exclusive, and more than one pattern could be present in the same patient.

Outcome Measures

The primary imaging discriminator was the presence of diffuse subendocardial LGE, considered characteristic of CA. Secondary imaging features included biatrial dilatation, pericardial/pleural effusion, alternative LGE patterns (transmural, mid-myocardial, subepicardial, patchy), and myocardial edema on T2 mapping.

Statistical Analysis

Distributional assumptions for continuous variables were assessed using the Shapiro-Wilk test. Continuous variables are reported as mean ± standard deviation when approximately normally distributed and compared using the Welch t-test; otherwise, they are presented as median (interquartile range) and compared using the Mann-Whitney U test. Categorical variables are summarized as n (%) and compared using Fisher's exact test. A two-sided $p<0.05$ was considered statistically significant. Given the pilot design, analyses were exploratory and no adjustment for multiple comparisons was applied.

Sample Size and Power Analysis

This study was retrospective, and the sample size was determined by the number of eligible patients undergoing CMR during the study period (December 2021-November 2025). A post-hoc power analysis was performed for the primary imaging discriminator, diffuse subendocardial LGE, using the observed proportions in the CA and non-amyloid groups (9/14 vs. 0/13). Assuming a two-sided $\alpha=0.05$, the achieved power to detect this difference was 0.998. In a conservative sensitivity analysis assuming a 10% prevalence of diffuse subendocardial LGE in the non-amyloid group, the achieved power was 0.885. Given the pilot design, other comparisons were considered exploratory.

Results

Study Population

A total of 27 patients were included in the final analysis: 14 with CA and 13 with non-amyloid inflammatory/fibrotic cardiac involvement. Within the non-amyloid group, diagnoses included cardiac sarcoidosis [5/13 (38.5%)], rheumatoid arthritis-related cardiac involvement [3/13 (23.1%)], SLE-associated myocarditis [3/13 (3.1%)], systemic sclerosis [1/13 (7.7%)], and endocardial fibroelastosis [1/13 (7.7%)].

Baseline Demographic and Clinical Characteristics

Baseline characteristics are summarized in Table 1. Patients with CA were older than those in the non-amyloid group (51.7±13.8 vs. 36.6±13.4 years, $p=0.008$). Sex distribution and the prevalence of hypertension and diabetes mellitus were similar between groups (all $p>0.05$). Pericardial and pleural effusions were more frequent in the non-amyloid group [pericardial effusion: 2/14 (14.3%) vs. 8/13 (61.5%), $p=0.018$; pleural effusion: 2/14 (14.3%) vs. 7/13 (53.8%), $p=0.046$].

CMR Morphological and Functional Findings

CMR morphological and functional parameters are presented in Table 2. Maximum left ventricle wall thickness, LV end-diastolic

Table 1. Baseline demographic and clinical characteristics of patients with cardiac amyloidosis and non-amyloid inflammatory/fibrotic cardiac involvement

Variable	Cardiac amyloidosis (n=14)	Non-amyloid inflammatory/fibrotic group (n=13)	p-value
Age, years (mean ± standard deviation)	51.7±13.8	36.6±13.4	**0.019**
Sex (male), n (%)	4 (28.6)	5 (38.5)	0.695
Hypertension, n (%)	7 (50.0)	5 (38.5)	0.704
Diabetes mellitus, n (%)	4 (28.6)	4 (30.8)	1.000
Pericardial effusion, n (%)	2 (14.3)	8 (61.5)	**0.018**
Pleural effusion, n (%)	2 (14.3)	7 (53.8)	**0.046**

Values are presented as mean ± standard deviation or number (percentage), as appropriate. Continuous variables were compared using the Welch t-test. Categorical variables were compared using Fisher's exact test (two-sided). A two-sided $p<0.05$ was considered statistically significant

volume (LVEDV), and LVEF did not differ significantly between groups (all p>0.05). Biatrial dilatation was more common in the CA group [10/14 (71.4%) vs. 2/13 (15.4%), p=0.006]. Right ventricle involvement was numerically more frequent in CA, but this difference did not reach statistical significance [5/14 (35.7%) vs. 1/13 (7.7%), p=0.165].

LGE Tissue Characterization Patterns

LGE distribution patterns differed significantly between groups (Table 2). CA was strongly associated with diffuse subendocardial LGE [9/14 (64.3%) vs. 0/13 (0%), p<0.001]. In contrast, the non-amyloid group more frequently demonstrated transmural [11/13 (84.6%) vs. 3/14 (21.4%), p=0.002], patchy [8/13 (61.5%) vs. 1/14 (7.1%), p=0.004], mid-myocardial [10/13 (76.9%) vs. 2/14 (14.3%), p=0.002], and subepicardial LGE [11/13 (84.6%) vs. 0/14 (0%), p<0.001]. Representative examples are shown in Figures 1, 2.

Myocardial Edema

Myocardial edema on T2 mapping was observed only in the non-amyloid group [0/14 (0%) vs. 4/13 (30.8%), p=0.041] (Table 2).

Descriptive Subgroup Findings

Given the limited number of patients within individual non-amyloid subgroups, analyses for specific diagnoses were descriptive. Cardiac sarcoidosis cases typically demonstrated patchy mid-myocardial and/or subepicardial LGE with associated myocardial edema. Rheumatoid arthritis-related and SLE-associated cases showed inflammatory enhancement patterns without the diffuse subendocardial LGE pattern characteristic of CA. Endocardial fibroelastosis was characterized by predominant endocardial involvement. In the non-amyloid cohort, transmural-appearing LGE was observed in 6/13 (46.2%) patients, contributed

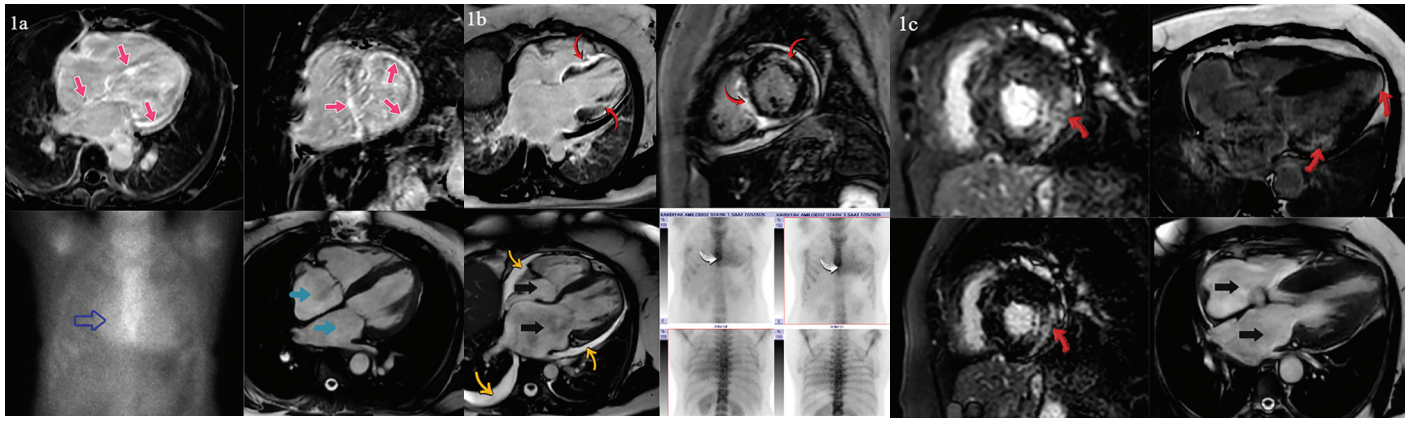

Figure 1. Representative CMR imaging LGE and bone scintigraphy findings in two patients with cardiac amyloidosis showing diffuse subendocardial enhancement and increased myocardial radiotracer uptake, (1a) In a 58-year-old woman, LGE images show diffuse subendocardial enhancement (pink arrows). Biatrial enlargement is also present (green arrows), and bone scintigraphy demonstrates increased myocardial radiotracer uptake (blue arrow), (1b) In a 62-year-old man patient, LGE demonstrates an atypical distribution with subendocardial, mid-myocardial, and subepicardial involvement (red arrows). Biatrial enlargement (black arrows) and pleural/pericardial effusions (yellow arrows) are noted. Bone scintigraphy again shows increased cardiac radiotracer uptake (white arrows), supporting the diagnosis of cardiac amyloidosis, (1c) In a 58-year-old woman with cardiac amyloidosis, LGE images demonstrate a predominantly subendocardial enhancement pattern (red arrows). Marked biatrial enlargement is also present (black arrows)

CMR: Cardic magnetic resonance, LGE: Late gadolinium enhancement

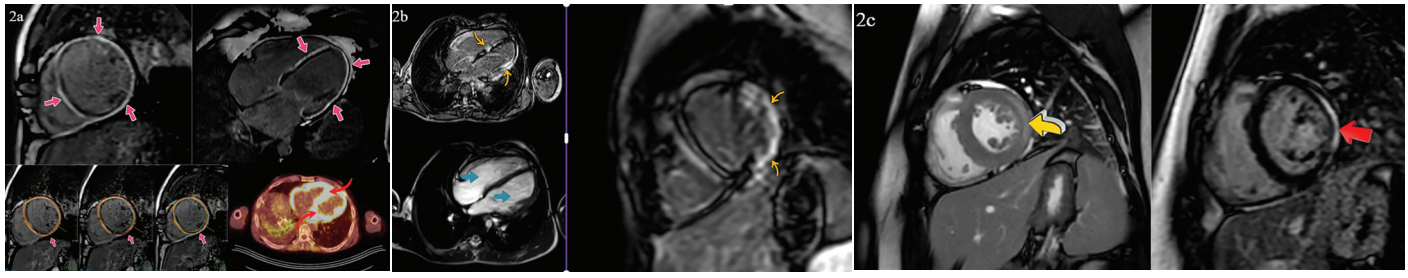

Figure 2. Representative CMR imaging patterns across non-amyloid inflammatory/fibrotic diagnoses (sarcoidosis, endocardial fibroelastosis, and systemic lupus erythematosus-associated myocarditis), highlighting subepicardial/mid-myocardial enhancement and edema on T2 mapping, (2a) In a 44-year-old man with cardiac sarcoidosis, late gadolinium enhancement images demonstrate diffuse subepicardial enhancement (pink arrows). Corresponding positron emission tomography/computed tomography shows increased myocardial fluorodeoxyglucose uptake (red arrow), consistent with active inflammatory involvement, (2b) In a 15-year-old boy with endocardial fibroelastosis, late gadolinium enhancement images show diffuse transmural and subepicardial enhancement (yellow arrows). Cine imaging demonstrates cardiomegaly (green arrow), (2c) In a 34-year-old woman with systemic lupus erythematosus, T2-weighted imaging demonstrates mid-myocardial edema in the lateral wall (yellow arrow), with corresponding LGE images (red arrow), consistent with myocarditis

CMR: Cardic magnetic resonance, LGE: Late gadolinium enhancement

mainly by cardiac sarcoidosis [2/5 (40.0%)], rheumatoid arthritis-related involvement [1/3 (33.3%)], SLE-associated myocarditis [1/3 (33.3%)], systemic sclerosis [1/1 (100%)], and endocardial fibroelastosis [1/1 (100%)]. Figure 2 provides representative CMR examples of characteristic patterns across disease categories.

Overall, CA and non-amyloid inflammatory/fibrotic cardiac diseases demonstrated distinct CMR patterns, particularly with respect to LGE distribution, atrial involvement, and the presence of myocardial edema, supporting the utility of CMR as a non-invasive tool for differentiating amyloid-related myocardial infiltration from inflammatory and fibrotic cardiac processes.

Discussion

In this single-center pilot study, we demonstrated that CMR reveals distinct and reproducible myocardial involvement patterns that enable differentiation between CA and non-amyloid inflammatory or fibrotic cardiac diseases. Despite overlapping clinical presentations and the shared classification of these entities as infiltrative cardiac conditions, their underlying pathophysiological mechanisms translated into markedly different CMR phenotypes.

The most important finding of our study was the strong association between CA and diffuse subendocardial LGE. This pattern is widely recognized as a hallmark of amyloid infiltration and reflects expansion of the extracellular space due to amyloid deposition.[1-3] Previous studies have reported that diffuse subendocardial LGE is highly suggestive of CA and correlates with disease burden and prognosis.[13] In our cohort, diffuse subendocardial LGE was observed exclusively in the CA group, whereas transmural LGE was more frequently encountered in the non-amyloid inflammatory/fibrotic group, underscoring the importance of interpreting LGE distribution together with edema and the overall clinical context.

Although transmural enhancement is often discussed in the context of advanced infiltrative disease, extensive inflammatory injury and fibrotic remodeling may also yield transmural-appearing LGE, particularly in severe or widespread myocarditis-like involvement and in fibrotic endocardial disorders. In our non-amyloid cohort, transmural LGE frequently co-occurred with subepicardial or patchy enhancement and with edema on T2 mapping, supporting an inflammatory/fibrotic mechanism rather than amyloid deposition. Therefore, we emphasize that differentiation should be based on a pattern-based interpretation, integrating LGE distribution, edema assessment, and associated morphological findings, rather than relying on a single LGE descriptor.[6-8]

In contrast, the non-amyloid group—including cardiac sarcoidosis, connective tissue disease-related myocardial involvement, inflammatory myocarditis, systemic sclerosis, and endocardial fibroelastosis—more commonly demonstrates patchy, mid-myocardial, and/or subepicardial LGE distributions, frequently accompanied by myocardial edema on T2-based imaging. This pattern aligns with prior CMR studies of inflammatory cardiomyopathies, in which immune-mediated myocardial injury typically results in focal or regional fibrosis and edema rather than diffuse extracellular infiltration.[7,8,14] Notably, cardiac sarcoidosis often shows heterogeneous enhancement patterns consistent with granulomatous inflammation and scarring, with common involvement of the basal septum and lateral wall.[10,15]

Table 2. CMR morphological and tissue characterization findings in cardiac amyloidosis versus non-amyloid inflammatory/fibrotic cardiac involvement, including LGE pattern distribution and T2 mapping-based edema

Variable	Cardiac amyloidosis (n=14)	Non-amyloid inflammatory/fibrotic group (n=13)	p-value
Morphological/functional findings			
Max LV wall thickness, mm	18.9	17.4	**0.410**
LV hypertrophy pattern (concentric), n (%)	10 (71.4)	7 (53.8)	**0.440**
LV end-diastolic volume (LVEDV), mL	105	88	**0.215**
LVEF, %	44	38	0.240
Biatrial dilatation (yes), n (%)	10 (71.4)	2 (15.4)	**0.006**
RV involvement (RV wall thickening and/or RV LGE), n (%)	5 (35.7)	1 (7.7)	0.165
Diffuse subendocardial LGE, n (%)	9 (64.3)	0 (0.0)	**<0.001**
Transmural LGE, n (%)	3 (21.4)	11 (84.6)	**0.002**
Patchy LGE, n (%)	1 (7.1)	8 (61.5)	**0.004**
Mid-myocardial LGE, n (%)	2 (14.3)	10 (76.9)	**0.002**
Subepicardial LGE, n (%)	0 (0.0)	11 (84.6)	**<0.001**
Myocardial edema on T2 (present), n (%)	0 (0.0)	4 (30.8)	**0.041**

Values are presented as n (%) or mean, as appropriate. Categorical variables were compared using Fisher's exact test (two-sided). Continuous variables were compared using [t-test/Mann-Whitney U] depending on distribution. LGE patterns were not mutually exclusive; more than one LGE pattern could be present in the same patient, LGE: Late gadolinium enhancement, RV: Right ventricle, CMR: Cardiac magnetic resonance imaging, LVEF: Left ventricular ejection fraction

The presence of myocardial edema emerged as another important discriminating feature. In our cohort, edema was largely absent in CA but commonly detected in inflammatory myocardial diseases, especially sarcoidosis and lupus-associated myocarditis. This observation aligns with existing literature emphasizing the value of T2-based imaging for identifying active myocardial inflammation.[12,16] The absence of edema in amyloidosis reflects the chronic, non-inflammatory nature of amyloid deposition and further supports the role of multiparametric CMR in differential diagnosis.

Morphological differences also contributed to diagnostic separation. Biatrial dilatation was significantly more common in CA, consistent with restrictive physiology and elevated filling pressures.[17,18] In our cohort, pericardial and pleural effusions were more frequently observed in the non-amyloid inflammatory/fibrotic group, which may reflect active inflammation and serosal involvement in systemic inflammatory diseases. Although effusions are non-specific, they can provide a supportive context when interpreted alongside LGE distribution and edema assessment.[11]

Our results support the concept that CMR pattern recognition, rather than reliance on a single imaging feature, offers the greatest diagnostic value in complex infiltrative and inflammatory cardiac diseases. While advanced techniques such as T1 mapping and extracellular volume (ECV) quantification have further improved tissue characterization in recent years,[19-21] our study demonstrates that even conventional CMR parameters, particularly LGE distribution and edema assessment, can provide meaningful diagnostic discrimination in routine clinical practice.

Study Limitations

Several limitations should be acknowledged. First, the retrospective single-center design is inherently subject to selection bias and limits causal inference. Second, the small sample size reduces statistical power; therefore, our analyses should be interpreted as exploratory and hypothesis-generating. Third, the non-amyloid comparator cohort was heterogeneous, intentionally reflecting real-world inflammatory and fibrotic myocardial involvement; however, this heterogeneity precluded robust subgroup-level statistical comparisons, which were reported descriptively. Fourth, there was an age imbalance between groups, which may have acted as a potential confounder and could influence myocardial remodeling and comorbidity profiles. Finally, although T2 mapping was available for edema assessment, advanced parametric mapping for diffuse myocardial characterization (e.g., native T1 mapping and ECV quantification) was not routinely performed, and LGE was evaluated visually without quantitative scar burden measurement. Larger prospective studies incorporating comprehensive multiparametric mapping and quantitative LGE assessment are warranted to validate and refine these findings.

Despite these limitations, our findings have important clinical implications. Early and accurate differentiation between CA and inflammatory or fibrotic myocardial disease is essential because management strategies diverge substantially. From a rheumatology perspective, systemic inflammatory disorders including autoinflammatory conditions may involve the myocardium and present with overlapping clinical features, underscoring the need for careful cardiac evaluation in inflammatory disease contexts.[22] In this setting, a pattern-based CMR approach can help identify inflammatory involvement while prompting targeted evaluation for CA when appropriate. This distinction is clinically critical, as disease-modifying therapies are now available for transthyretin amyloidosis, whereas inflammatory conditions often require immunosuppression and targeted arrhythmia management.[4,6,23] Misclassification may delay appropriate treatment and adversely affect outcomes.

Conclusion

This pilot study demonstrates that CMR provides distinct and complementary imaging patterns that facilitate differentiation of CA from non-amyloid inflammatory and fibrotic cardiac involvement. Recognition of characteristic LGE distribution, assessment of myocardial edema (including T2 mapping), and evaluation of associated morphological features can enhance diagnostic confidence and support disease-specific management. Larger prospective studies incorporating comprehensive multiparametric tissue characterization and quantitative assessment are warranted to further validate and refine these findings.

Ethics

Ethics Committee Approval: Ethical approval was obtained from the Non-Interventional Clinical Research Ethics Committee of Aydın Adnan Menderes University Faculty of Medicine (approved number: 07-2025/377, date: 18.12.2025).

Informed Consent: Informed consent was waived due to the retrospective design and use of anonymized data.

Footnotes

Authorship Contributions

Concept: G.T., Design: G.T., A.A., Data Collection and Processing: G.T., A.A., Analysis and Interpretation: G.T., A.A., Literature Search: A.A., Writing: G.T.

Conflict of Interest: No conflict of interest was declared by the authors.

Financial Disclosure: The authors declare that they have no relevant financial disclosures.

References

1. Falk RH, Alexander KM, Liao R, Dorbala S. AL (light-chain) amyloidosis: cardiac involvement and treatment. J Am Coll Cardiol. 2016;68:1323-41.
2. Banypersad SM, Moon JC, Whelan C, Hawkins PN, Wechalekar AD. Updates in cardiac amyloidosis: a review. J Am Heart Assoc. 2012;1:e000364.
3. Maceira AM, Joshi J, Prasad SK, et al. Cardiovascular magnetic resonance in cardiac amyloidosis. Circulation. 2005;111:186-93.
4. Maurer MS, Schwartz JH, Gundapaneni B, et al. Tafamidis treatment for patients with transthyretin amyloid cardiomyopathy. N Engl J Med. 2018;379:1007-16.
5. Fontana M, Pica S, Reant P, et al. Prognostic value of late gadolinium enhancement cardiovascular magnetic resonance in cardiac amyloidosis. Circulation. 2015;132:1570-9.
6. Birnie DH, Nery PB, Ha AC, Beanlands RS. Cardiac sarcoidosis. J Am Coll Cardiol. 2016;68:411-21.
7. Friedrich MG, Sechtem U, Schulz-Menger J, et al. Cardiovascular magnetic resonance in myocarditis: a JACC White Paper. J Am Coll Cardiol. 2009;53:1475-87.
8. Ferreira VM, Schulz-Menger J, Holmvang G, et al. Cardiovascular magnetic resonance in nonischemic myocardial inflammation: Expert recommendations. J Am Coll Cardiol. 2018;72:3158-76.
9. Tzelepis GE, Kelekis NL, Plastiras SC, Mitseas P, Economopoulos N, Moyssakis I. Pattern and distribution of myocardial fibrosis in systemic sclerosis: a delayed enhanced MRI study. Arthritis Rheum. 2007;56:3827-36.
10. Patel MR, Cawley PJ, Heitner JF, et al. Detection of myocardial damage in patients with sarcoidosis. Circulation. 2009;120:1969-77.
11. Syed IS, Glockner JF, Feng D, et al. Role of cardiac magnetic resonance imaging in the detection of cardiac amyloidosis. J Am Coll Cardiol Img. 2010;3:155-64.
12. Abdel-Aty H, Zagrosek A, Schulz-Menger J, et al. Delayed enhancement and T2-weighted cardiovascular magnetic resonance imaging differentiate acute from chronic myocardial infarction. Circulation. 2004;109:2411-6.
13. Vogelsberg H, Mahrholdt H, Deluigi CC, et al. Cardiovascular magnetic resonance in clinically suspected cardiac amyloidosis. J Am Coll Cardiol. 2008;51:1022-30.
14. Lurz P, Eitel I, Adam J, et al. Diagnostic performance of CMR imaging compared with EMB in patients with suspected myocarditis. J Am Coll Cardiol. 2012;59:755-63.
15. Greulich S, Deluigi CC, Gloekler S, et al. CMR imaging predicts death and other adverse events in suspected cardiac sarcoidosis. J Am Coll Cardiol Img. 2013;6:501-11.
16. Ferreira VM, Piechnik SK, Dall'Armellina E, et al. Native T1 mapping detects the location, extent and patterns of acute myocarditis. J Cardiovasc Magn Reson. 2014;16:36.
17. Martinez-Naharro A, Hawkins PN, Fontana M. Cardiac amyloidosis. Clin Med (Lond). 2018;18(Suppl 2):s30-5.
18. Banypersad SM, Sado DM, Flett AS, et al. Quantification of myocardial extracellular volume fraction in systemic amyloidosis. J Am Coll Cardiol Img. 2013;6:34-9.
19. Karamitsos TD, Piechnik SK, Banypersad SM, et al. Noncontrast T1 mapping for the diagnosis of cardiac amyloidosis. J Am Coll Cardiol Img. 2013;6:488-97.
20. Fontana M, Banypersad SM, Treibel TA, et al. Native T1 mapping in transthyretin amyloidosis. J Am Coll Cardiol Img. 2014;7:157-65.
21. Moon JC, Messroghli DR, Kellman P, et al. Myocardial T1 mapping and extracellular volume quantification. J Cardiovasc Magn Reson. 2013;15:92.
22. Gunay Y, Karagozlu F, Gemici S, et al. Examination of cardiac functions during acute attack and remission period in children with familial Mediterranean fever. Eur J Pediatr. 2024;183:3137-45.
23. Gilstrap LG, Dominici F, Wang Y, et al. Epidemiology of cardiac amyloidosis-associated heart failure hospitalizations. Circulation. 2019;140(2):170-80.